Journal of Materials Science and Chemical Engineering, 2026, 14(2), 1-14
https://www.scirp.org/journal/msce
ISSN Online: 2327-6053
ISSN Print: 2327-6045

Study of the Glass System, $(100 - x)(3K_2S - 7P_2S_5) - xKI$ (x = 0, 5, 10, 15, and 20) for K^+ Ion Conductivity

Ram Krishna Hona[1]*, Carl White[1], Md. Sofiul Alom[2]

[1]Environmental Science Department, United Tribes Technical College, Bismarck, ND, USA
[2]Department of Chemistry, Dhaka University of Engineering and Technology, Gazipur, Bangladesh
Email: *rhona@uttc.edu

How to cite this paper: Hona, R.K., White, C. and Alom, Md.S. (2026) Study of the Glass System, $(100 - x)(3K_2S - 7P_2S_5) - xKI$ (x = 0, 5, 10, 15, and 20) for K^+ Ion Conductivity. *Journal of Materials Science and Chemical Engineering*, **14**, 1-14.
https://doi.org/10.4236/msce.2026.142001

Received: December 30, 2025
Accepted: February 6, 2026
Published: February 9, 2026

Abstract

A series of glassy electrolytes in the ternary system $(100 - x)(3K_2S - 7P_2S_5) - xKI$ (x = 0, 5, 10, 15 and 20) was investigated, with a focus on their potassium-ion conductivity using electrochemical impedance spectroscopy (EIS). Among the compositions studied, the electrolyte with x = 20 exhibited the highest ambient-temperature conductivity, measured at 2.36×10^{-10} S·cm^{-1}. The materials were characterized by XRD, DSC, and Raman spectroscopy. DSC results revealed glass transition temperatures just above 130˚C; therefore, temperature-dependent conductivity measurements were performed within the range of 21˚C - 125˚C to determine activation energies without interference from thermal transitions. Raman spectroscopic analysis confirmed the presence of invariant structural units of the network former— PS_4^{3-}, PS_7^{4-}, PS_6^{4-} —across all glassy electrolytes. The similarity of vibrational modes to those of the parent composition indicates that halide ions do not interact chemically with these network-forming units. Instead, the halide ions occupy interstitial sites within the glass structure. The observed increase in ionic conductivity with higher KI content is attributed to a rise in charge carrier concentration, consistent with the interstitial incorporation of halide ions without disrupting the anionic framework.

Keywords

XRD, Solid-State Reaction, Glass Electrolytes, Impedance Spectroscopy, Raman Spectra

1. Introduction

Potassium batteries (such as K-ion battery, K-sulfur battery and K-O_2 battery) have gained considerable attention in recent years due to low cost, abundant resources, and relatively low reduction potential [1]-[3]. It has been reported that potassium batteries can deliver higher energy storage capacity and energy density relative to Li– and Na– batteries [2] [3]. However, since the liquid electrolyte containing commercially available batteries posed risks of leakage, flammability and electrode corrosion, attention has been diverted to the development of all-solid-state batteries (ASSB) [4] [5] which are considered the safest energy storage systems because of the nonflammable and electrochemically stable solid state electrolytes [6]. Since the performance of a battery is rooted in the nature of the electrodes and electrolyte [7], it is important to have an electrolyte of good quality in a K– battery in addition to its cathode and anode. The introduction of high quality solid electrolyte reflects the efficiency of a battery with high energy density, capacity and durability. For this reason, the search for electrolyte materials with high K^+ ionic conductivity at ambient temperature is a key step toward developing all-solid-state batteries with high energy and power densities [8].

The increasing research interest in developing all solid-state K-batteries necessitated high room temperature K^+-ion conducting solid electrolytes. Attempts could be seen at developing different types of electrolytes such as solid polymer [9] [10] and inorganic electrolytes of different classes and phases [11] [12] for solid state K-battery. Inorganic solid electrolytes have been the focus of investigation [11]-[13]. Most of the studied inorganic solid electrolytes include mixed ionic and electronic conductivity [13]-[16]. For all solid state potassium batteries (K-ion or K-S or KO_2 batteries), purely K^+ ion conducting electrolyte which has no electronic conductivity is required. Among the different classes of purely K^+ ion conducting inorganic solid electrolytes, ionic glass/ amorphous electrolyte is one of the potential electrolytes. Ag^+ and Li^+ ions conducting glassy electrolytes have proved that the conductivity of glass electrolyte can be comparable to that of liquid electrolyte that is required for a room temperature battery operation. [17]-[19] Glasses are isotropic, without grain boundaries and are easy to fabricate in the form of complex shapes that can be used to optimize the properties due to wide compositional flexibility. Much attention has been paid to the studies of the ionic glasses with Li^+ and Na^+ conductivity [20]-[23]. However, there has been less attention in the study of K^+ ion conducting glassy electrolyte. Because of the larger ionic volume of K^+ ion relative to Li^+ and Na^+ ions, achieving glassy solid electrolytes with high K^+ ionic conductivity is a major challenge for the design and synthesis. Though, reports of mixed ions (such as K^+, Li^+, Na^+, etc.) conducting glasses can be found [24] [25], only a handful of reports can be found to have been studied until today which reported only one and pure K^+ ion conducting glass electrolyte [12] [26]-[29]. Among the 5 published reports [12] [26]-[29] we have found, only one report mentioned the room temperature purely K^+ ion conductivity which is close to 10^{-10} S·cm^{-1} [27].

In general, inorganic alkali ionic glass is composed of glass network former and glass modifier. Network formers are the compounds of covalent nature such as oxides and sulfides of Si, P and B and glass modifiers are the compounds of ionic natures such as oxides and sulfides of alkali metals. Modifiers break the network of long chain to build the pathways for cation movement from one spot to another. This makes a glass ion conductive. However, salts are added to improve the ionic conductivity [30] in glasses. Generally, the added salts are alkali halides or oxyanion salts of the alkali metals, such as MX, M_2SO_4, M_4SiO_4 (M = Li, Na, K and x = Cl, Br, I) etc. [31]-[35]. Sometimes nitrides are also added [36]. We added potassium iodide in the glassy electrolytes. The conventional alkali ionic glasses were generally synthesized by melt quench technique at higher temperature (>700˚C) [20] [37]. We also followed the conventional method for the synthesis of our glass system, $(100 - x)(3K_2S - 7P_2S_5) - xKI$ (x = 0, 5, 10, 15 and 20).

2. Experimental

Glassy electrolytes were synthesized from three chemicals: K_2S (95%, Strem Chemicals), P_2S_5 (99.99%, Alfa Aesar) and KI (99.99%, Alfa Aesar) as starting materials at different compositions. Before their use, all the chemicals were dried at 120˚C for 2 days. Stoichiometric amount of each chemical was weighed for each composition. They were mixed homogeneously in mortar and pestle and kept in a quartz tube which was sealed later on. All the work was done in argon environment inside a glovebox. The quartz tube was then taken out of the glovebox and vacuum sealed and heated to 700˚C for 3 hours. It was quenched in liquid nitrogen. The phase purity and glass formation were characterized by powder X-ray diffraction using Brucker D8 ADVANCE with X-ray diffractometer copper Kα-radiation device (1.5418 Å). Since the samples were air sensitive, the materials were covered with 3M film to collect the XRD data. The data were collected between 2θ of 10 and 60 degrees. Differential scanning calorimetry (DSC) method was used to characterize the glass transition temperatures. The measurements were carried out in the temperature range from 0˚C to 380˚C in Al pans with a heating rate of 10˚C min^{-1} in dry Argon atmosphere using DSC Q200-1776. Raman spectra were collected using a 514/613 nm Argon laser on a Reinshaw inVia Spectrometer scanning from 100 to 800 cm^{-1} with a 50x objective lens. 10 accumulations are taken per sample lasting 20 seconds each in length. Because the samples were susceptible to hygroscopic attack, they were contained in glass capillary tube and sealed with a sealant. The ionic conductivities of the glass samples were investigated by electrical impedance spectroscopy (EIS) using Gamry reference 600 potentiostat. Impedance measurements were performed in the frequency range 0.1 Hz to 1 MHz using a computer-controlled frequency response analyzer. For the measurements, pellets of as synthesized materials were pressed into a disc of 6 mm diameter using a pressure of 2 tons. The pellets were coated with Pt spray on both sides using plasma sputtering for 6 minutes on each side. This platinum coating acts as current collector and electrodes. The pellet was kept in an air sealed Swagelok cell. The whole setting of the pellet in Swagelok cell was performed inside glovebox and the AC impedance measurement was performed outside the glovebox in an

MTI 1100 box furnace. The pellet in the Swagelok cell was first sintered at 125˚C for 4 hours to bring the particles into close packing and then the impedance measurement was started from 21˚C to 125˚C.

3. Results and Discussion

3.1. Synthesis and Characterization

The glassy electrolytes of the compositions (100 − x)($3K_2S - 7P_2S_5$) − xKI (x = 0, 5, 10, 15 and 20) were prepared by conventional quenching. The powdered materials were characterized by powder X-ray diffraction. All the compositions showed no peaks in the X-ray diffraction conforming the formation of the glassy/amorphous materials. Figure 1 Shows the powder X-ray diffraction of the glassy electrolytes (100 – x)($3K_2S - 7P_2S_5$) – xKI (x = 0, 5, 10, 15 and 20). Since the materials were very hygroscopic and sensitive to air, the samples were covered by 3M film during the X-ray data collection. The peaks of the 3M film were intense and appeared between 2θ of 26 and 29 degrees. To avoid the interference or confusion of the peaks in the data, they were cut off. The materials were also characterized by differential scanning calorimetry (DSC). DSC data were collected between 0 and 380˚C. Figure 2(a) shows the DSC data for x = 0, 5, 10, 15 and 20. The relation of glass transition temperature with the compositions is shown in Figure 2(b). The Tg increases with the increase of KI salt in the glassy electrolyte until x = 15. However, the Tg value decreases after x = 15. Since the DSC data shows a peak near 180˚C, XRD data were collected after heat treatment of a sample at two different temperatures to figure out the cause of the peak. For this, first a pure glass composition of x = 20 was prepared by quenching at 700˚C. Then the same sample was divided into two portions. One was heated to 125˚C and the other was heated to 180˚C. The heating rate was 5˚C/minute and the cooling was natural. The sample heated to 125˚C did not show impurity peak but the one heated to 180˚C showed the impurity peaks in XRD data as shown in Figure 3. The Peak in DSC data near 180˚C should be therefore due to the phase change from glass to glass ceramic.

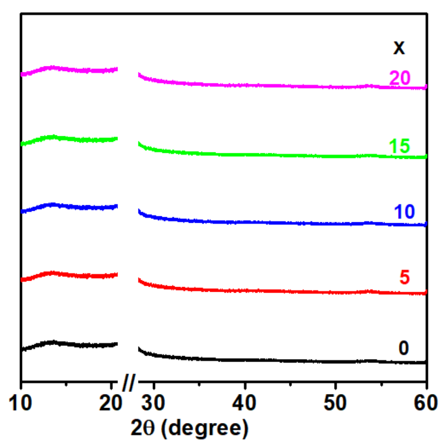

Figure 1. Powder X-ray diffraction of the glassy electrolytes (100 – x)($3K_2S - 7P_2S_5$) – xKI (x = 0, 5, 10, 15 and 20).

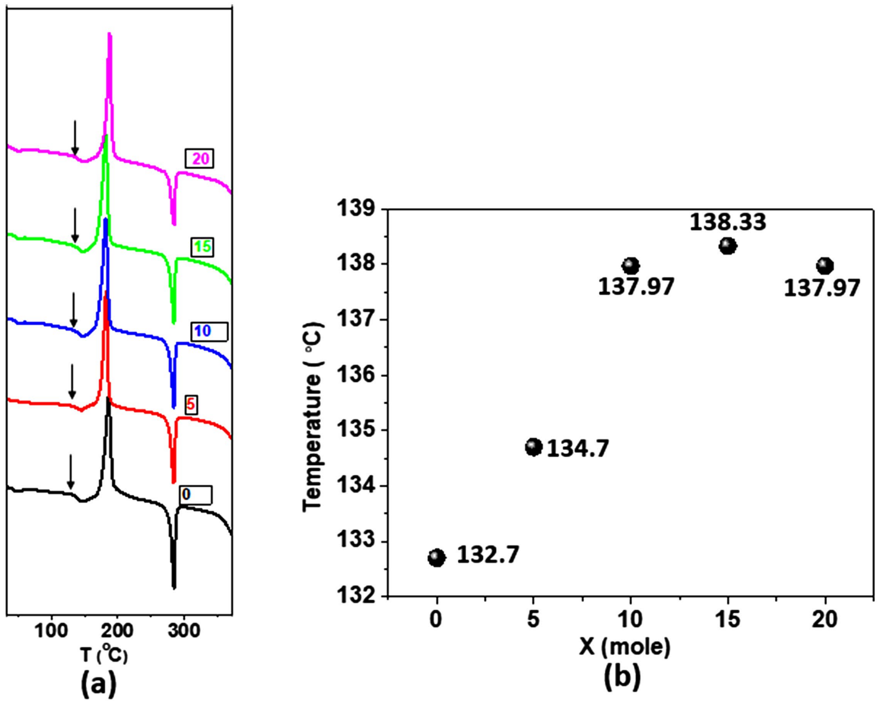

Figure 2. DSC data of (100 − x)($3K_2S - 7P_2S_5$) − xKI (x = 0, 5, 10, 15 and 20). (a) The arrows show the glass transition temperature (Tg). Tg were taken at the onset of the slope in all samples. (b) Tg as a function of x (mole).

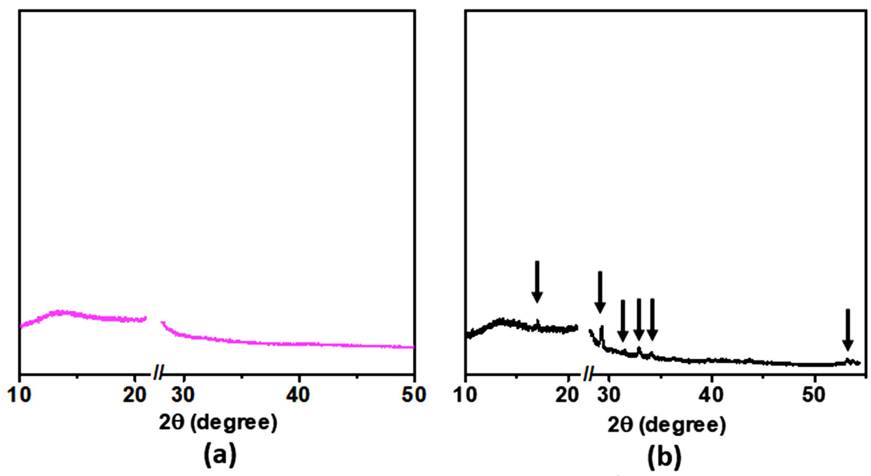

Figure 3. Powder XRD of (100 − x)($3K_2S - 7P_2S_5$) − xKI (x = 20) collected at room temperature after sintering to (a) 125˚C and (b) 180˚C for 2 hours and then cooled naturally.

Figure 4 shows the Raman spectra of the electrolytes. In the Raman spectra, x = 0, 5, 10 and 15 show the similar data but 20 differs from them; specifically, $P_2S_6^{4-}$ peak splits and new peaks appear. These new peaks are not known to attribute to which species. According to the previous report of Li-analog, the similarity of vibrational modes with parent composition indicates the non-interaction of halide ion with network former units and reside interstitially in the glass system [38].

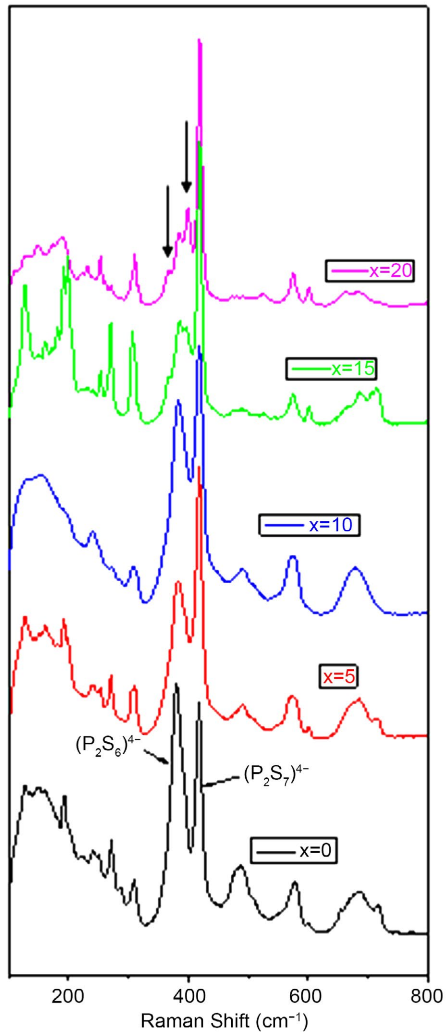

Figure 4. Raman data of (100 − x)($3K_2S - 7P_2S_5$) − xKI (x = 0, 5, 10, 15 and 20).

3.2. Conductivity

ASSB requires purely ion conducting electrolyte. Ionic conductivity of an electrolyte can be determined by EIS studies. We measured the impedance of a series of glassy electrolytes using EIS within the frequency range of 0.1 Hz to 1 MHz. To determine the highest temperature limit for conductivity measurement at variable temperature, differential scanning calorimetry (DSC) data were collected for the series of the electrolytes which showed the glass transition temperatures just above 130˚C and another peak near 180˚C. To analyze the peak at 180˚C, XRD data was collected after heating the glass at 180˚C for 2 hours which exhibited peaks (**Figure 3(b)**) conforming the phase transformation. Glassy electrolytes lose their properties after phase transition temperature. Since the glass transition temperatures were just above 130˚C, the conductivities of the glasses were measured below 130˚C within the temperature range of 21˚C to 125˚C. Generally, impedance is measured at low voltage (10 - 100 mV). However, different problems are observed to apply low voltage to measure impedance for a material with very high impedance [39]. So, high voltage is used to measure high impedance of a solid material [40]. Our materials exhibited the impedance of several GΩ at room temperature. So, we used different voltage ranging from 20 to 200 mV to measure the impedance of the studied materials depending on the impedance of the materials. We also tested for one of our materials with different voltage from 20 mV to 500 mV for the impedance. There is no difference in the magnitude of real and imaginary part of the impedance data. For most of the materials, 20 mV was used. Glass is lack of grain boundaries. The ideal EIS of glasses with ionic conductivity exhibit a semicircle. When the impedance of a glass is measured as an electrolyte, bulk resistance from bulk material, capacitive effect of the bulk and the double layer capacitance at the interface of the electrode and material can be considered. Hence, we used an equivalent circuit for our materials as shown in inset of **Figure 5** where R1 and R2 represent resistance of wire (lead) and the bulk material, respectively and CPE1 and CPE2 represent the capacitance of the bulk material and the electrode electrolyte double layer capacitive behavior, respectively [41]. Constant phase element (CPE) is generally applied for nonideal capacitive behavior which is demonstrated by imperfect semicircle. The nonideal behavior is considered to be caused by surface roughness, leakage capacitance, and nonuniform distribution [41]. In our materials (**Figure 5**), depressed semicircles with heights smaller than half of their diameter were observed. Thus, the classical parallel R//C circuit which is used for perfect semicircle with the center located on the real axis in the Nyquist diagram is not the suitable equivalent circuit to model this type of glasses. **Figure 5** shows a fitted impedance data of x = 20˚C at 100˚C as a representative of the compositions $(100 - x)(3K_2S - 7P_2S_5) - xKI$ (x = 0, 5, 10, 15 and 20). The inset demonstrates the equivalent circuit used. The black circles represent the raw data and the red stars represent the fitted data. The observed curve shows the typical ionic conductivity behavior containing a high-frequency semicircle which represent the bulk properties of the material and the low frequency tail is the response of interfacial (electrode) polarization [42]. Some of the studied materials did not show the tail region at room temperature which might be due to frequency limitation as it showed the high resistivity. The semicircle without spike observation at lower temperature for some materials is not surprising. It has been observed for other materials in the past reports [43]-[45]. The intercept of the semicircular curve on the low frequency region gives the resistance of a material under study. This resistance (R) is used to determine the conductivity (σ) of the bulk material (circular pellet) by the application of its thickness (L) and surface area (A) as given in the relation 1 [46].

$$\sigma = \frac{L}{RA} \tag{1}$$

In the series of materials, the room temperature ionic conductivity increases with the increase of KI concentration. Li and Na based chalcogenide glasses were also reported to increase ionic conductivity with the addition of halide ion and its concentration. The increase of ionic conductivity is attributed to the increase of charge carriers with the increase of the halide ions [38] [47]. Handful of reports can be found for the study of K^+ ion conductivity of glassy electrolytes of which only one paper reported the room temperature K^+ ion conductivity [48] [49]. Among the studied glassy electrolytes of our study, the electrolyte with x = 20 demonstrated the highest room temperature K^+ ion conductivity with 2.36 x 10^{-10} $S\cdot cm^{-1}$. **Table 1** shows the room temperature K^+ ion conductivity and Ea of the glassy electrolytes $(100 - x)(3K_2S - 7P_2S_5) - xKI$ (x = 0, 5, 10, 15 and 20). The room temperature conductivity order for X is 20 >15 - 10 > 5 > 0.

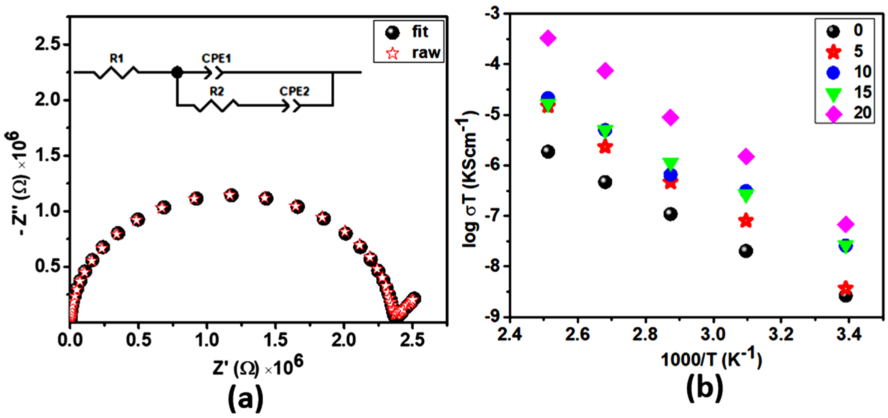

Figure 5. (a) Representative Impedance data of x = 20 at 100˚C with inset of equivalence circuit used for fitting and (b) Conductivity of $(100 - x)(3K_2S - 7P_2S_5) - xKI$ (x = 0, 5, 10, 15 and 20).

Table 1. Conductivity at 21 ˚C and Ea values of $(100 - x)(3K_2S - 7P_2S_5) - xKI$ (x = 0, 5, 10, 15 and 20).

X	σ_{21} ($S\cdot cm^{-1}$)	E_a (eV)
0	9.18E−12	0.65
5	3.15E−11	0.83
10	8.72E−11	0.64
15	8.32E−11	0.64
20	2.36E−10	0.81

The studies of temperature dependent conductivity of glassy electrolytes can also characterize their nature. Thus, almost all of our glassy electrolytes studied for their ionic conductivities were studied for their conductivities at variable temperatures ranging from ambient to high temperature. Temperature dependent conductivities of all of the studied glasses were measured from 21˚C to 125˚C. All electrolytes exhibited the semiconductive nature by decreasing resistivity with the increase of temperature within the measured temperature range. The measurement was stopped at 125˚C because the glassy electrolytes showed the glass transition temperature just above this temperature. It is found that the conductivity is higher for higher KI concentration at all temperature except for x = 10 and 15. The conductivities overlap at almost all temperatures for these two compositions.

From these experiments the activation energies were obtained, as shown in Table 1. The conductivity trends and the Arrhenius plots for the series of glasses are shown in Figure 5(b). The plot in Figure 5(b) was used for fitting with the Arrhenius equation for thermally activated conductivity [46] (shown in Equation (2)) which helped to find the activation energy.

$$\sigma T = \sigma^0 e^{-\frac{E_a}{kT}} \tag{2}$$

where σ^0 is a pre-exponential factor and a characteristic of a material, and E_a, k, and T are the activation energy for the conductivity, Boltzmann constant, and absolute temperature, respectively. The activation energy (E_a) can be calculated from slope of the lines of best fit in the log σT vs 1000/T plot.

Raman Spectroscopic Analysis

Raman spectroscopy was used to examine the structural units present in the $(100 - x)(3K_2S - 7P_2S_5) - xKI$ glass system (x = 0, 5, 10, 15 and 20) and to assess the effect of KI addition on the glass network. The Raman spectra of all compositions show characteristic vibrational bands corresponding to PS_7^{4-}, and PS_6^{4-} units, which are well-known network-forming species in alkali thiophosphate glasses. The presence of these units across all compositions confirms that the basic thiophosphate glass network remains intact upon KI incorporation.

No significant shifts in Raman peak positions or the appearance of new bands are observed with increasing KI content, indicating that KI addition does not cause major structural modifications of the network former units. This suggests that iodide ions do not chemically interact with the thiophosphate network but instead reside interstitially within the glass matrix, consistent with earlier reports on halide-doped glass electrolytes.

For the composition with x = 20, an additional Raman band corresponding to the PS_4^{3-} unit is observed. The formation of PS_4^{3-} units indicate partial network depolymerization and an increase in non-bridging sulfur species, which can facilitate alkali-ion transport. This structural feature correlates with the highest K^+ ion concentration and the maximum room-temperature ionic conductivity of 2.36 x 10^{-10} S·cm^{-1} observed for this composition.

Overall, the Raman results confirm that the enhancement in K^+ ion conductivity with increasing KI content is primarily due to the increased charge carrier concentration rather than changes in the glass network structure, with the emergence of PS_4^{3-} units at higher KI content providing a favorable local environment for improved ionic conduction.

4. Conclusion

The study of the ternary glass system $(100 - x)(3K_2S - 7P_2S_5) - xKI$ (x = 0, 5, 10, 15 and 20) demonstrates that the addition of KI does not lead to significant structural modification of the thiophosphate glass network. Raman spectroscopic analysis confirms the presence of PS_7^{4-}, and PS_6^{4-} structural units in all compositions, indicating that the fundamental network structure is preserved. The similarity of vibrational modes with the parent composition further suggests that iodide ions do not interact with the network former units and are accommodated interstitially within the glass matrix.

The K^+ ion conductivity increases systematically with increasing KI content, which is primarily attributed to the enhanced charge carrier concentration. Among the studied compositions, the glass with x = 20 exhibits the highest room-temperature ionic conductivity of 2.36×10^{-10} S·cm^{-1}, consistent with its highest K^+ ion concentration. In addition, the appearance of the PS_4^{3-} structural unit exclusively in the x = 20 composition indicates partial network depolymerization, leading to the formation of non-bridging sulfur species. The presence of PS_4^{3-} units is likely to facilitate K^+ ion transport by creating a more open structural environment and favorable conduction pathways.

Overall, the enhanced ionic conductivity observed with increasing KI addition arises from the combined effect of increased mobile K^+ ion concentration and the formation of PS_4^{3-} units at higher KI content, while the thiophosphate glass network remains largely unchanged.

Acknowledgments

This work is partly supported by the National Science Foundation Tribal College and University Program Instructional Capacity Excellence in TCUP Institutions (ICE-TI) grant award #2225648. NSF TCUP Tribal Enterprise Advancement Center supports a part of this work, grant no. HRD 1839895. A part of the work is supported by AIHEC-coordinated NASA TCU Building Bridges, Grant Number 80NSSC24M0025. Additional support for the work came from ND EPSCOR STEM equipment grants. Permission was granted by the United Tribes Technical Colleges (UTTC) Environmental Science Department to publish this information. The views expressed are those of the authors and do not necessarily represent those of United Tribes Technical College.

Conflicts of Interest

The authors declare no conflict of interest.

References

[1] Rajagopalan, R., Tang, Y., Ji, X., Jia, C. and Wang, H. (2020) Advancements and Challenges in Potassium Ion Batteries: A Comprehensive Review. *Advanced Functional Materials*, **30**, Article 1909486. https://doi.org/10.1002/adfm.201909486

[2] Zhu, Y.H., Yin, Y.B., Yang, X., Sun, T., Wang, S., *et al.* (2017) Transformation of Rusty Stainless-Steel Meshes into Stable, Low-Cost, and Binder-Free Cathodes for High-Performance Potassium-Ion Batteries. *Angewandte Chemie International Edition*, **56**, 7881-7885. https://doi.org/10.1002/anie.201702711

[3] Hosaka, T., Kubota, K., Hameed, A.S. and Komaba, S. (2020) Research Development on K-Ion Batteries. *Chemical Reviews*, **120**, 6358-6466. https://doi.org/10.1021/acs.chemrev.9b00463

[4] Fei, H., Liu, Y., An, Y., Xu, X., Zeng, G., Tian, Y., *et al.* (2018) Stable All-Solid-State

Potassium Battery Operating at Room Temperature with a Composite Polymer Electrolyte and a Sustainable Organic Cathode. *Journal of Power Sources*, **399**, 294-298. https://doi.org/10.1016/j.jpowsour.2018.07.124

[5] Fei, H., Liu, Y., An, Y., Xu, X., Zhang, J., Xi, B., *et al.* (2019) Safe All-Solid-State Potassium Batteries with Three Dimentional, Flexible and Binder-Free Metal Sulfide Array Electrode. *Journal of Power Sources*, **433**, Article 226697. https://doi.org/10.1016/j.jpowsour.2019.226697

[6] Wang, Y., Song, S., Xu, C., Hu, N., Molenda, J. and Lu, L. (2019) Development of Solid-State Electrolytes for Sodium-Ion Battery—A Short Review. *Nano Materials Science*, **1**, 91-100. https://doi.org/10.1016/j.nanoms.2019.02.007

[7] Reddy, M.V., Subba Rao, G.V. and Chowdari, B.V.R. (2013) Metal Oxides and Oxysalts as Anode Materials for Li Ion Batteries. *Chemical Reviews*, **113**, 5364-5457. https://doi.org/10.1021/cr3001884

[8] Yuan, H., Li, H., Zhang, T., Li, G., He, T., Du, F., *et al.* (2018) A $K_2Fe_4O_7$ Superionic Conductor for All-Solid-State Potassium Metal Batteries. *Journal of Materials Chemistry A*, **6**, 8413-8418. https://doi.org/10.1039/c8ta01418c

[9] Chandra, A., Basak, S., Khan, M.Z., Chandra, A., Dhundhel, R.S. and Bhatt, A. (2020) Synthesis and Ionic Conductivity Measurement of a New Potassium Ion Conducting Solid Polymer Electrolytes. *IOP Conference Series: Materials Science and Engineering*, **798**, Article 012007. https://doi.org/10.1088/1757-899x/798/1/012007

[10] Kesharwani, P., Sahu, D.K., Mahipal, Y.K. and Agrawal, R.C. (2017) Conductivity Enhancement in K+-Ion Conducting Dry Solid Polymer Electrolyte (SPE): [PEO: KNO3]: A Consequence of KI Dispersal and Nano-Ionic Effect. *Materials Chemistry and Physics*, **193**, 524-531. https://doi.org/10.1016/j.matchemphys.2017.03.015

[11] Yamamoto, S., Tamura, S. and Imanaka, N. (2006) New Type of Potassium Ion Conducting Solid Based on Lanthanum Oxysulfate. *Journal of Alloys and Compounds*, **418**, 226-229. https://doi.org/10.1016/j.jallcom.2005.10.064

[12] Fusco, F.A., Massot, M., Oueslati, M., Haro, E., Tuller, H.L. and Balkanski, M. (2011) Structural Changes in Fast Ion Conducting Chloride Doped Potassium Borate Glasses. *MRS Proceedings*, **135**, 189-197. https://doi.org/10.1557/proc-135-189

[13] Burmakin, E.I., Nechaev, G.V. and Shekhtman, G.S. (2007) Solid Potassium-Cation-Conducting Electrolytes in the $K_{1-2x}Ba_xFeO_2$ and $K_{1-2x}Pb_xFeO_2$ Systems. *Russian Journal of Electrochemistry*, **43**, 121-124. https://doi.org/10.1134/s1023193507010181

[14] Burmakin, E.I., Antonov, B.D. and Shekhtman, G.S. (2010) Potassium Ion Conducting $K_{1-2x}Cd_xFeO_2$ Solid Electrolytes. *Inorganic Materials*, **46**, 540-544. https://doi.org/10.1134/s0020168510050183

[15] Burmakin, E.I. and Shekhtman, G.S. (2008) Potassium Ion Conducting $K_{2-2x}Fe_{2-x}P_xO_4$ Solid Electrolytes. *Inorganic Materials*, **44**, 882-885. https://doi.org/10.1134/s0020168508080189

[16] Nechaev, G.V. and Burmakin, E.I. (2011) Potassium-Conducting $K_{1-2x}Pb_xGaO_2$ Solid Electrolytes. *Russian Journal of Electrochemistry*, **47**, 457-460. https://doi.org/10.1134/s1023193511040112

[17] Braga, M.H., Ferreira, J.A., Stockhausen, V., Oliveira, J.E. and El-Azab, A. (2014) Novel Li_3ClO Based Glasses with Superionic Properties for Lithium Batteries. *Journal of Materials Chemistry A*, **2**, 5470-5480. https://doi.org/10.1039/c3ta15087a

[18] Braga, M.H., Murchison, A.J., Ferreira, J.A., Singh, P. and Goodenough, J.B. (2016) Glass-Amorphous Alkali-Ion Solid Electrolytes and Their Performance in Symmetrical Cells. *Energy & Environmental Science*, **9**, 948-954.

https://doi.org/10.1039/c5ee02924d

[19] Minami, T., Imazawa, K. and Tanaka, M. (1980) Formation Region and Characterization of Superionic Conducting Glasses in the Systems AgI-Ag_2O-M_xO_y. *Journal of Non-Crystalline Solids*, **42**, 469-476. https://doi.org/10.1016/0022-3093(80)90045-9

[20] Jha, P.K., Pandey, O. and Singh, K. (2013) Na_2S-P_2S_5 Based Super-Ionic Glasses for Solid Electrolytes. *Transactions of the Indian Ceramic Society*, **72**, 5-9. https://doi.org/10.1080/0371750x.2013.793999

[21] Startsev, Y.K., Pronkin, A.A., Sokolov, I.A. and Murin, I.V. (2011) Electrical Conductivity and Structure of Glasses in the Na_2O-Na_2S-P_2O_5 and Na_2S-P_2S_5 Systems. *Glass Physics and Chemistry*, **37**, 263-282. https://doi.org/10.1134/s1087659611030138

[22] Kulkarni, A.R., Maiti, H.S. and Paul, A. (1984) Fast Ion Conducting Lithium Glasses—Review. *Bulletin of Materials Science*, **6**, 201-221. https://doi.org/10.1007/bf02743897

[23] Chandra, A., Bhatt, A. and Chandra, A. (2013) Ion Conduction in Superionic Glassy Electrolytes: An Overview. *Journal of Materials Science & Technology*, **29**, 193-208. https://doi.org/10.1016/j.jmst.2013.01.005

[24] Lodesani, F., Menziani, M.C., Hijiya, H., Takato, Y., Urata, S. and Pedone, A. (2020) Structural Origins of the Mixed Alkali Effect in Alkali Aluminosilicate Glasses: Molecular Dynamics Study and Its Assessment. *Scientific Reports*, **10**, Article No. 2906. https://doi.org/10.1038/s41598-020-59875-7

[25] Narasimham, P.S.L., Mahadevan, S. and Rao, K.J. (1979) Electrical Conductivity Studies in K_2SO_4-$ZnSO_4$ Glasses. *Indian Academy of Sciences*, **88**, 11-17. https://doi.org/10.1007/bf02863251

[26] Budina, D., Zakel, J., Martin, J., Menezes, P., Schäfer, M. and Weitzel, K. (2014) Bombardment Induced Transport of Rb+ through a K^+ Conducting Glass vs. K^+ Transport through a Rb^+ Conducting Glass. *Zeitschrift für Physikalische Chemie*, **228**, 609-627. https://doi.org/10.1515/zpch-2014-0459

[27] Yao, W. and Martin, S. (2008) Ionic Conductivity of Glasses in the Mi + M_2S + ($0.1Ga_2S_3$+$0.9GeS_2$) System (m=Li, Na, K and Cs). *Solid State Ionics*, **178**, 1777-1784. https://doi.org/10.1016/j.ssi.2007.10.011

[28] Thipperudra, A., Nagaraja, N., Prashanth Kumar, M. and Arunkumar, B. (2020) DSC and FTIR Studies in Potassium, Strontium Doped Boro-Phosphate Glasses. *Chemistry and Materials Research*, **12**, 1-8.

[29] Lejeune, M., Colomban, P. and Boilot, J.P. (1982) Fast Potassium Ion Conduction in Quenched KASICON Glass. *Journal of Non-Crystalline Solids*, **51**, 273-276. https://doi.org/10.1016/0022-3093(82)90011-4

[30] Lau, J., DeBlock, R.H., Butts, D.M., Ashby, D.S., Choi, C.S. and Dunn, B.S. (2018) Sulfide Solid Electrolytes for Lithium Battery Applications. *Advanced Energy Materials*, **8**, Article 1800933. https://doi.org/10.1002/aenm.201800933

[31] Kennedy, J.H. (1989) Ionically Conductive Glasses Based on SiS_2. *Materials Chemistry and Physics*, **23**, 29-50. https://doi.org/10.1016/0254-0584(89)90015-1

[32] Hirai, K., Tatsumisago, M. and Minami, T. (1995) Thermal and Electrical Properties of Rapidly Quenched Glasses in the Systems Li_2S-SiS_2-Li_xMO_y (Li_xMO_y=Li_4SiO_4, Li_2SO_4). *Solid State Ionics*, **78**, 269-273. https://doi.org/10.1016/0167-2738(95)00094-m

[33] Deshpande, V.K. (2004) Factors Affecting Ionic Conductivity in the Lithium Conducting Glassy Solid Electrolytes. *Ionics*, **10**, 20-26. https://doi.org/10.1007/bf02410300

[34] Kondo, S., Takada, K. and Yamamura, Y. (1992) New Lithium Ion Conductors Based on Li_2S-SiS_2 System. *Solid State Ionics*, **53**, 1183-1186. https://doi.org/10.1016/0167-2738(92)90310-l

[35] Tatsumisago, M., Hirai, K., Hirata, T., Takahashi, M. and Minami, T. (1996) Structure and Properties of Lithium Ion Conducting Oxysulfide Glasses Prepared by Rapid Quenching. *Solid State Ionics*, **86**, 487-490. https://doi.org/10.1016/0167-2738(96)00179-8

[36] Munoz, F., Duran, A., Pascual, L., Montagne, L., Revel, B. and Rodrigues, A. (2008) Increased Electrical Conductivity of Lipon Glasses Produced by Ammonolysis. *Solid State Ionics*, **179**, 574-579. https://doi.org/10.1016/j.ssi.2008.04.004

[37] Kennedy, J.H. and Yang, Y. (1986) A Highly Conductive Li^+-Glass System: (1 − X) ($0.4SiS_2$ − $0.6Li_2S$) − xLil. *Journal of the Electrochemical Society*, **133**, 2437-2438. https://doi.org/10.1149/1.2108425

[38] Mercier, R., Malugani, J., Fahys, B. and Robert, G. (1981) Superionic Conduction in Li_2S-P_2S_5-Lii-Glasses. *Solid State Ionics*, **5**, 663-666. https://doi.org/10.1016/0167-2738(81)90341-6

[39] Brisebois, G. (2016) Signal Conditioning for High-Impedance Sensors EDN.

[40] Whittam, J., Hector, A.L., Kavanagh, C., Owen, J.R. and Reid, G. (2018) Combination of Solid-State and Electrochemical Impedance Spectroscopy to Explore Effects of Porosity in Sol-Gel-Derived $BaTiO_3$ Thin Films. *ACS Omega*, **3**, 6880-6887. https://doi.org/10.1021/acsomega.8b00173

[41] Choi, W., Shin, H., Kim, J.M., Choi, J. and Yoon, W. (2020) Modeling and Applications of Electrochemical Impedance Spectroscopy (EIS) for Lithium-Ion Batteries. *Journal of Electrochemical Science and Technology*, **11**, 1-13. https://doi.org/10.33961/jecst.2019.00528

[42] Shimakawa, K. (2019) Electrical Transport Properties of Glass. In: *Springer Handbooks*, Springer, 343-367. https://doi.org/10.1007/978-3-319-93728-1_10

[43] Jha, P.K., Pandey, O.P. and Singh, K. (2016) Non-Isothermal Crystallization Kinetics of K_2O Modified Sodium-Phosphate Glasses. *Journal of Non-Crystalline Solids*, **440**, 76-84. https://doi.org/10.1016/j.jnoncrysol.2016.03.002

[44] Liu, X., Liang, B., Zhang, M., Long, Y. and Li, W. (2017) Enhanced Photocatalytic Properties of A-Snwo4 Nanosheets Modified by Ag Nanoparticles. *Journal of Colloid and Interface Science*, **490**, 46-52. https://doi.org/10.1016/j.jcis.2016.11.029

[45] Montouillout, V., Fan, H., del Campo, L., Ory, S., Rakhmatullin, A., Fayon, F., *et al.* (2018) Ionic Conductivity of Lithium Borate Glasses and Local Structure Probed by High Resolution Solid-Sate NMR. *Journal of Non-Crystalline Solids*, **484**, 57-64. https://doi.org/10.1016/j.jnoncrysol.2018.01.020

[46] Neyret, M., Lenoir, M., Grandjean, A., Massoni, N., Penelon, B. and Malki, M. (2015) Ionic Transport of Alkali in Borosilicate Glass. Role of Alkali Nature on Glass Structure and on Ionic Conductivity at the Glassy State. *Journal of Non-Crystalline Solids*, **410**, 74-81. https://doi.org/10.1016/j.jnoncrysol.2014.12.002

[47] Hibi, Y., Tanibata, N., Hayashi, A. and Tatsumisago, M. (2015) Preparation of Sodium Ion Conducting Na_3PS_4-NaI Glasses by a Mechanochemical Technique. *Solid State Ionics*, **270**, 6-9. https://doi.org/10.1016/j.ssi.2014.11.024

[48] Hona, R.K., Azure, A.D., Guinn, M., Phuyal, U.S., Stroh, K. and Thapa, A.K. (2023) Ionic Conductivity of K-Ion Glassy Solid Electrolytes of K_2S-P_2S_5-Kotf System. *International Journal of Molecular Sciences*, **24**, Article 16855. https://doi.org/10.3390/ijms242316855

[49] Hona, R.K., Guinn, M., Phuyal, U.S., Sanchez, S. and Dhaliwal, G.S. (2023) Alkali Ionic Conductivity in Inorganic Glassy Electrolytes. *Journal of Materials Science and Chemical Engineering*, **11**, 31-72. https://doi.org/10.4236/msce.2023.117004